JACS
JOURNAL OF THE AMERICAN CHEMICAL SOCIETY

Article

pubs.acs.org/JACS

Universal Correlation between Fibril Width and Quantum Efficiency in Diketopyrrolopyrrole-Based Polymer Solar Cells

Weiwei Li, Koen H. Hendriks, Alice Furlan, W. S. Christian Roelofs, Martijn M. Wienk, and René A. J. Janssen*

Molecular Materials and Nanosystems, Eindhoven University of Technology, P.O. Box 513, 5600 MB Eindhoven, The Netherlands

Supporting Information

ABSTRACT: For a series of six diketopyrrolopyrrole (DPP)-based conjugated polymers, we establish a direct correlation between their external quantum efficiencies (EQE) in organic solar cells and the fibrillar microstructure in the blend. The polymers consist of electron-deficient DPP units, carrying long branched 2′-decyltetradecyl (DT) side chains for solubility, that alternate along the main chain with electron-rich aromatic segments comprising benzene, thiophene, or fused aromatic rings. The high molecular weight DT-DPP polymers were incorporated in bulk heterojunction solar cells with [6,6]-phenyl-C_{71}-butyric acid methyl ester ([70]PCBM) as acceptor. The morphology of the DT-DPP:[70]PCBM blends is characterized by a semicrystalline fibrillar microstructure with fibril widths between 4.5 and 30 nm as evidenced from transmission electron microscopy. A clear correlation is found between the widths of the fibrils and the EQE for photon to electron conversion. The highest EQEs (60%) and power conversion efficiencies (7.1%) are obtained for polymers with fibril widths less than 12 nm. For blends with fibrils wider than 12 nm, the EQE is low because exciton diffusion becomes limiting for charge generation. Interestingly, the correlation found here matches with previous data on related DPP-based polymers. This suggests that for this class of materials the relation between fiber width and EQE is universal. The fiber width is largely correlated with the solubility of the polymers, with less soluble DPP-based polymers giving narrower fibrils.

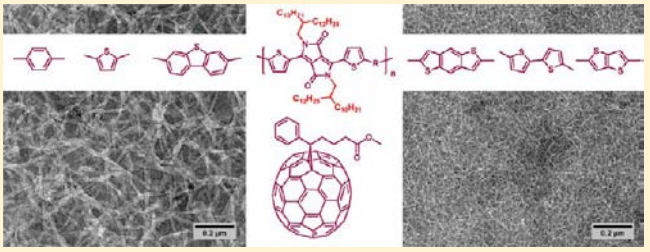

1. INTRODUCTION

In the past 5 years, diketopyrrolopyrrole (DPP)-based polymers have emerged as a promising class of semiconducting polymers for organic solar cells.[1−18] The small optical band gap and high charge carrier mobility of DPP-based polymers enable achieving high power conversion efficiencies (PCEs) up to 8% when mixed with [70]PCBM ([6,6]-phenyl-C_{71}-butyric acid methyl ester).[19] Their significant absorption in the near-infrared (NIR) region has made DPP-based polymers a preferred class of materials for use in the small band subcell of multijunction solar cells that reach efficiencies up to 9.6%.[20−28]

In designing materials for polymer solar cells it is well established that apart from the chemical structure, which determines the optical band gap and energy levels, the morphology of the photoactive donor−acceptor blend plays a crucial role.[29−32] The blend morphology is determined by the chemical structure and by the processing conditions used to cast the layers. Important processing parameters are donor/acceptor ratio, solvent, cosolvent, temperature, drying time, and concentration. At present, our understanding of the interplay between these parameters is rather phenomenological. Although theoretical models that rationalize morphology formation are being developed,[33] a quantitative description of the relation between chemical structure and optimized blend morphology is missing. In part, this is caused by the fact that few studies exist that quantitatively correlate chemical structure to morphology for a range of related materials.

Recently, we found a notable example of a correlation between the chemical structure, the optimized morphology, and the solar cell performance among a homologous series of DPP-based polymers in blends with [70]PCBM.[34] For three high molecular weight PDPPTPT polymers, we established that the PCE significantly increases, from 3.2% to 7.4%, when the length of the solubilizing branched alkyl side chains decreases. Interestingly, these PDPPTPT derivatives form semicrystalline polymer fibrils of different widths in blends with [70]PCBM. The length of the side chains correlates with the width of the fibrils. If the fibril is significantly wider than the exciton diffusion length, less charges are formed, and the external quantum efficiency (EQE) for photon to electron conversion and, consequently, the PCE are reduced.

This result suggests that for DPP-based polymers, there might be a more general relation between fibril width and EQE. Based on results for related DPP polymers available from previous work,[18] we suspected that the relation between the side chain length and width of the DPP polymer fibrils is not simply a geometric one, but rather linked to the solubility they impart on the polymer. Longer side chains increase the solubility, which

Received: October 1, 2013
Published: November 27, 2013

dx.doi.org/10.1021/ja4101003 | J. Am. Chem. Soc. 2013, 135, 18942−18948

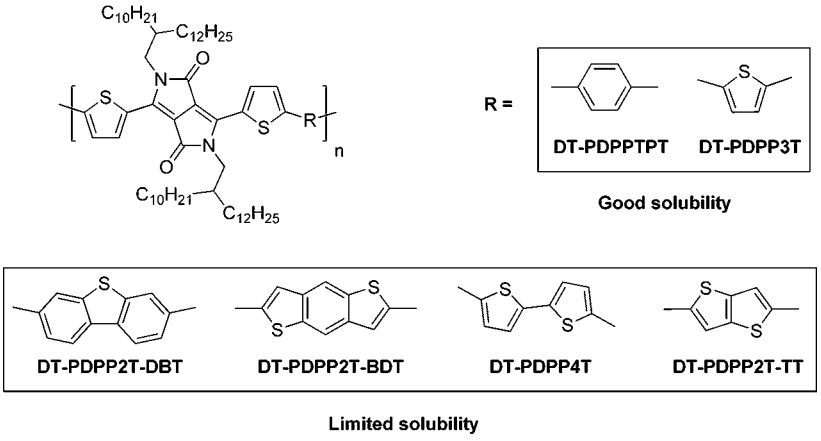

Figure 1. Diketopyrrolopyrrole-based conjugated polymers with decyltetradecyl (DT) substituents described in this work.

Scheme 1. Polymerization Reactions Used for DT-DPP Polymers[a]

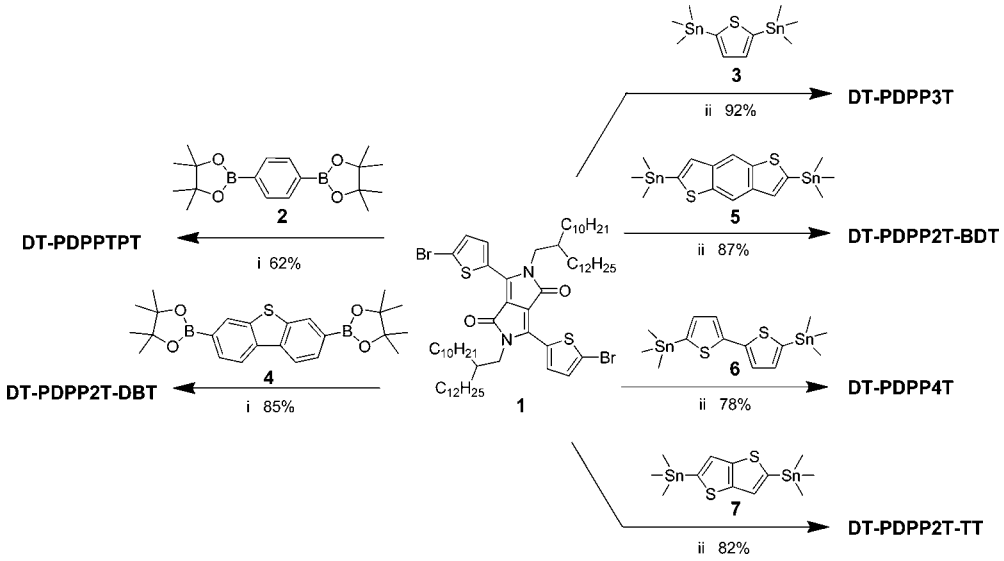

[a](i) Suzuki polymerization using $Pd_2(dba)_3/PPh_3/K_3PO_4$ (aq)/Aliquat 336 in toluene at 115 °C. (ii) Stille polymerization using $Pd_2(dba)_3/PPh_3$ in toluene/DMF (10:1, v/v) at 115 °C.

Table 1. Molecular Weight, Optical, and Electrochemical Properties of the DT-DPP Polymers

polymer	M_n (kg/mol)[a]	M_w (kg/mol)[a]	PDI	E_g^{sol} (eV)	E_g^{film} (eV)	E_{red} (V)[b]	E_{ox} (V)[b]	E_g^{CV} (eV)	α (eV)[c]
DT-PDPPTPT	89.2	215.6	2.42	1.57	1.54	−1.51	0.17	1.68	0.44
DT-PDPP3T	136.8	457.5	3.34	1.43	1.36	−1.50	0.02	1.52	0.43
DT-PDPP2T-DBT	149.9	552	3.68	1.66	1.62	−1.51	0.13	1.64	0.44
DT-PDPP2T-BDT[d]				1.53	1.51	−1.42	0.13	1.55	0.35
DT-PDPP4T	218.5	640.5	2.93	1.43	1.43	−1.59	−0.14	1.45	0.52
DT-PDPP2T-TT[d]				1.41	1.39	−1.55	−0.13	1.42	0.48

[a]Determined with GPC at 80 °C using *o*-DCB as the eluent. [b]Versus Fc/Fc^+. [c]$\alpha = e(E_{red}([70]PCBM) - E_{red})$ with $E_{red}([70]PCBM) = -1.07$ V vs Fc/Fc^+. [d]Part of the GPC trace appeared earlier than the polystyrene calibration limit molecular weight of 6035 kg/mol.

results in more time being available for the crystalline fibers to grow during film formation and hence wider fibers.

To test the idea that solubility rather than side chain length itself is important for the width of the fibrils and the solar cell performance, we now compare a series of high molecular weight DPP-based polymers that all have the same extended 2′-decyltetradecyl (DT) side chains, but differ in their backbone. The DT-DPP polymers consists of bis(2-thienyl)pyrrolo[3,4-*c*]pyrrolo-1,4-dione units with DT side chains that alternate along the polymer backbone with different electron rich aromatic linkers that do not carry any solubilizing side chains (Figure 1). Hence, larger aromatic linkers result in a decreased solubility. The polymers were applied in bulk heterojunction solar cells with [70]PCBM as acceptor and provided PCEs ranging from 3.2% to 7.1%. Transmission electron microscopy (TEM) reveals that the fibril width varied from 4.5 to 30 nm and correlates with the EQE in the high wavelength (λ > 700 nm) region. For blends with fibrils wider than 12 nm, the EQE is low because exciton diffusion and charge generation become limiting. We demonstrate that the highest EQEs and PCEs are obtained for polymers with limited

dx.doi.org/10.1021/ja4101003 | J. Am. Chem. Soc. 2013, 135, 18942−18948

solubility for which the fibril width in blends with [70[PCBM is less than 12 nm.

2. RESULTS AND DISCUSSION

The DT-DPP-based polymers were prepared by Suzuki or Stille polymerization (Scheme 1). The synthesis of three derivatives, DT-PDPPTPT, DT-PDPP3T, and DT-PDPP2T-TT, has been described previously.[18,34] A catalyst system based on $Pd_2(dba)_3$ as source of palladium with PPh_3 as ligand was found to give high reactivity. For the Stille polymerizations, a toluene/DMF (10:1, v/v) solvent mixture was used to obtain high molecular weight materials. The Suzuki couplings were performed in toluene/water mixtures.

The molecular weight of the polymers has been determined by gel permeation chromatography (GPC) using *o*-dichlorobenzene (*o*-DCB) as eluent. To reduce aggregation, the GPC column was held at 80 °C and the polymer concentration was reduced to 0.06 mg/mL. As shown in Table 1 and Figure 2, all polymers gave high molecular weights up to M_n = 220 kg/mol. For the polymers with benzodithiophene (BDT) and thienothiophene (TT) units, part of GPC traces exceed the calibration limit of the polystyrene standard of 6035 kg/mol such that the molecular weight cannot be determined (Table 1). The asymmetric shape of the GPC traces of these two polymers suggest that these polymers are aggregated under the analysis conditions. The generally very high molecular weights obtained for the DT-DPP polymers evidence an efficient polymerization reaction. The high molecular weight enhances the tendency to form aggregates in films, which can be beneficial for organic photovoltaic devices.

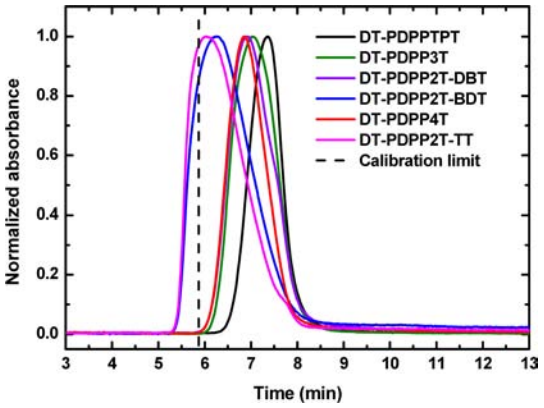

Figure 2. GPC traces of the DT-DPP polymers with *o*-DCB as eluent at 80 °C. The dashed line indicates the calibration limit of the column (PL-GEL 10 μm MIXED-B) with the polystyrene standard of 6035 kg/mol.

The different electron-donating units used in this work modulate the onsets of absorption in the 750−900 nm range for the polymers dissolved in chloroform (see Supporting Information (SI): Figure S1). All polymers exhibit a red-shifted absorption in thin solid films compared to chloroform solution (Figure 3a and Table 1), but the shifts are relatively small. This indicates that the polymers are likely already aggregated in solution. In thin films, DT-PDPP2T-DBT (i.e., having dibenzothiophene units) gives the highest band gap of 1.54 eV, while DT-PDPP3T (i.e., with thiophene units) gives the smallest band gap of 1.36 eV.

The oxidation and reduction potentials of the polymers have been determined electrochemically by cyclic voltammetry (CV) with the polymer in an *o*-DCB-based electrolyte (Table 1, Figure 3b, and SI Figure S2). The electrochemical band gaps determined from the onset of the oxidation and reduction waves in the CV measurements are a little higher than the optical band gaps in chloroform (Table 1). The differences are larger (~0.10 eV) for the two more soluble polymers and smaller (≤0.04 eV) for the four less soluble materials, suggesting that in the latter case aggregation occurs in both chloroform and *o*-DCB. The offset α (or LUMO−LUMO offset) between the reduction potentials of the polymers and that of [70]PCBM ranges from 0.35 to 0.52 V, which is smaller than for the polymers with extended conjugated units that we reported recently.[15]

The charge carrier mobility of the conjugated polymers has been determined in field-effect transistors (FETs) with a bottom-contact bottom-gate configuration and a passivated SiO_2 gate dielectric (SI Table S2). The DT-substituted DPP polymers with benzene and dibenzothiophene give limited hole mobilities ($10^{-3} < \mu_h < 10^{-2}$ cm^2/(V s)). The other polymers provide satisfying saturated hole mobilities of $\mu_h \geq 4 \times 10^{-2}$ cm^2/(V s). We note that these charge carrier mobilities are strongly dependent on the precise device configuration. In a FET with a bottom-contact top-gate configuration and a PMMA dielectric, DT-PDPP2T-TT provides a significantly higher value of $\mu_h = 8 \times 10^{-1}$ cm^2/(V s), resulting from an improved charge injection and a better dielectric interface.[18]

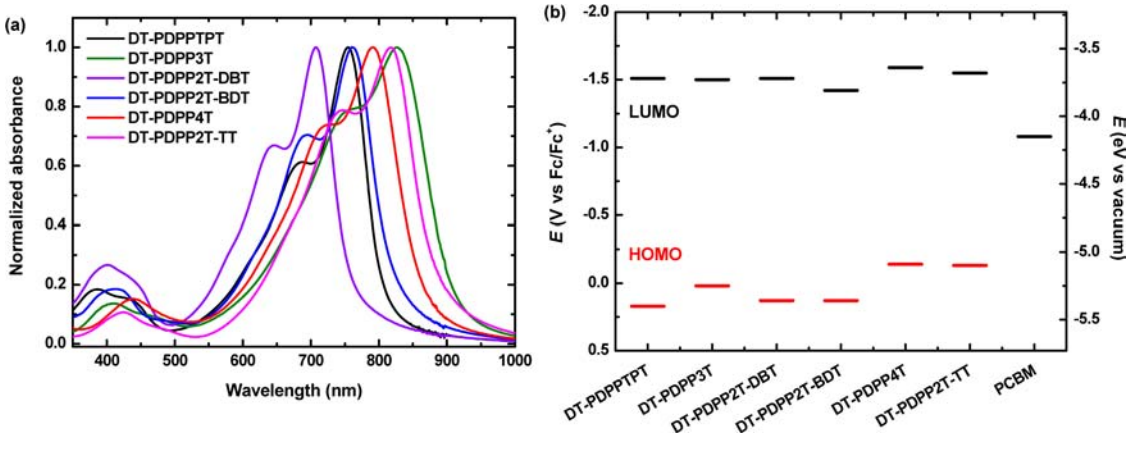

Figure 3. (a) Electronic absorption spectra of the DPP polymers in solid state films. (b) Energy levels determined from cyclic voltammetry (E(Fc/Fc$^+$) = −5.23 eV).

dx.doi.org/10.1021/ja4101003 | J. Am. Chem. Soc. 2013, 135, 18942−18948

Table 2. Characteristics of Optimized Solar Cells of the DT-DPP Polymers with [70]PCBM

polymer	solvent	d (nm)	J_{sc} (mA/cm^2)[a]	V_{oc} (V)	FF	PCE (%)[a]	EQE[b]	w (nm)	solubility[c]
DT-PDPPTPT[d]	$CHCl_3$:DIO 5%	100	6.6	0.81	0.59	3.2	0.24	30	+
DT-PDPP3T[d]	$CHCl_3$:DIO 5%	240	10.6	0.65	0.71	4.8	0.21	29	+
DT-PDPP2T-DBT[d]	$CHCl_3$:*o*-DCB 20%	90	10.2	0.76	0.68	5.3	0.44	9	−
DT-PDPP2T-BDT[d]	$CHCl_3$:*o*-DCB 10%	110	13.2	0.77	0.68	6.9	0.51	6.3	−
DT-PDPP4T[d]	$CHCl_3$:*o*-DCB 7.5%	115	16.0	0.64	0.69	7.1	0.60	4.5	−
DT-PDPP2T-TT[e]	$CHCl_3$:*o*-DCB 7.5%	220	14.8	0.66	0.70	6.9	0.35	17	−

[a] J_{sc} was calculated by integrating the EQE spectrum with the AM1.5G spectrum. [b] Maximum EQE in the wavelength region > 700 nm. [c] Solublity in chloroform. [d] Content ratio of the polymers to [70]PCBM is 1:2. [e] Content ratio of the polymers to [70]PCBM is 1:3.

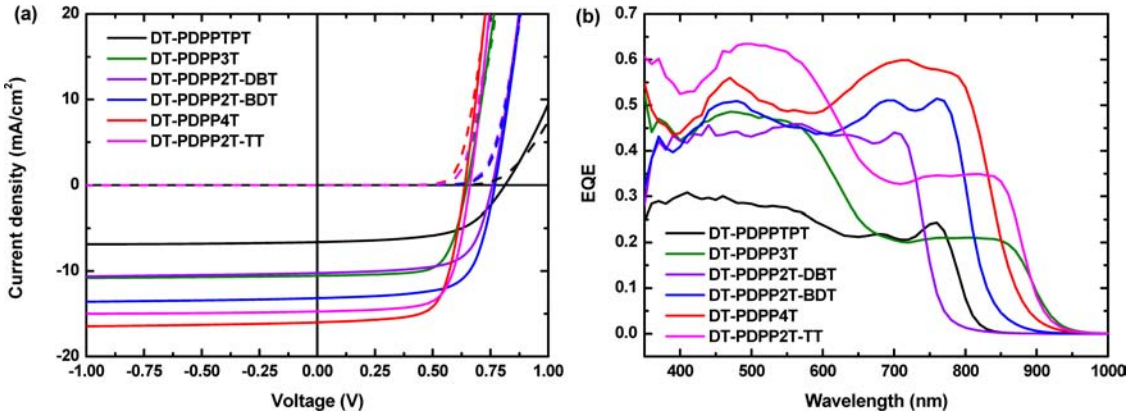

Figure 4. (a) $J-V$ characteristics in dark (dashed lines) and under white light illumination (solid lines) of optimized solar cells of the DPP polymers with [70]PCBM. (b) EQE of the same devices.

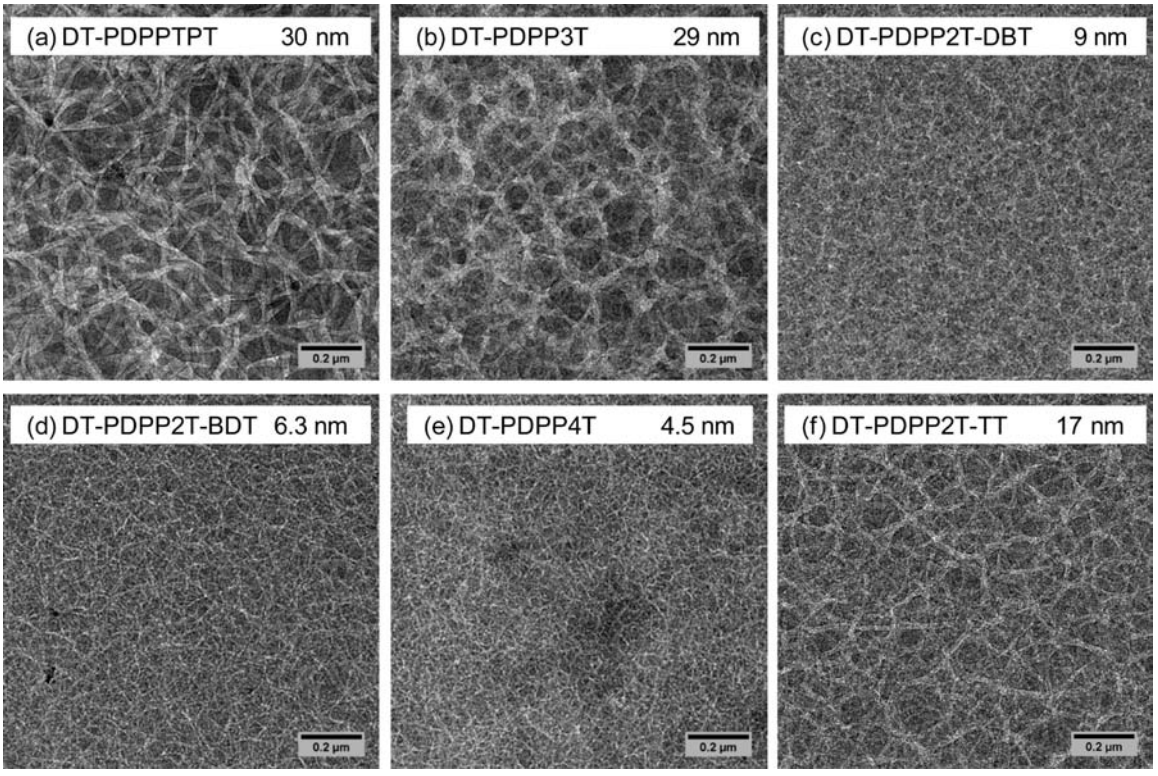

Figure 5. (a–f) Bright field TEM images ($1.2 \times 1.2\ \mu m^2$) of the optimized DPP polymer:[70]PCBM blend films. The average width of the fibrils (w) is indicated in the legends. The scale bar in the TEM images is 200 nm.

Solar cells were made by blending the DT-DPP polymers with [70]PCBM. The photoactive layer was sandwiched between transparent ITO/PEDOT:PSS and reflective LiF/Al back electrodes. Several device and processing parameters such as the polymer to [70]PCBM weight ratio, the active layer thickness (SI Figures S3, S4 and Tables S3, S4), the processing solvent, and the processing additive (1,8-diiodooctane (DIO) or *o*-DCB) concentration were carefully optimized. For blends of DT-

dx.doi.org/10.1021/ja4101003 | J. Am. Chem. Soc. 2013, 135, 18942−18948

PDPPTPT and DT-PDPP3T with [70]PCBM the highest PCEs were achieved for 5% DIO in chloroform. For lower DIO concentrations, the PCE decreases, while with 7.5% or 10% DIO the results were similar to those obtained with 5% DIO. Spin-coating these blends from chloroform with *o*-DCB or from pure *o*-DCB resulted in PCEs lower than 1%. The optimized processing conditions and layer thicknesses (d) are collected in Table 2 together with the solar cell characteristics. The current density−voltage (J−V) characteristics and external quantum efficiency (EQE) values are shown in Figure 4. The PCEs vary from 3.2% to 7.1%.

Except for DT-PDPPTPT all materials show excellent fill factors (FF) close to FF = 0.7. The highest photocurrent (16.0 mA/cm^2) is found for DT-PDPP4T, which results from a high EQE close to 0.6 in the polymer absorption region (Figure 4b). Compared to related DPP derivatives with the shorter OD (2′-octyldodecyl) side chains, a substantial enhancement has been established by using DT. Russell et al.[17] reported for OD-PDPP4T PCE = 5.6%, compared to PCE = 7.1% that we find for the DT analogue. A similar increase is seen for OD-PDPP2T-BDT, where Jo et al.[8] reported PCE = 5.2%, compared to PCE = 6.9% we find now for the same material but with DT side chains. An even more dramatic improvement is achieved for DT-PDPP2T-TT (PCE = 6.9%) where previously reported PCEs with HD (2′-hexyldecyl) or OD side chains did not exceed 2%.[5,9] However, the longer DT side chains do not always give better performance. Actually, the DT-substituted polymers with the smaller benzene and thiophene, DT-PDPPTPT and DT-PDPP3T, only gave PCEs of 3.2% and 4.8% as a consequence of low photocurrents, and performed significantly less than the PCEs of 7.4% and 7.1% for the polymers HD-PDPPTPT and HD-PDPP3T prepared using the same polymerization method.[19]

The morphology of the optimized DT-DPP:[70]PCBM photoactive layers was investigated with TEM (Figure 5) and atomic force microscopy (AFM, SI Figures S5 and S6). The TEM images show a distinct fibrillar structure for each of the blends, but the widths of the fibrils (w) are clearly different. The width is less than 10 nm for the active layers of [70]PCBM blended with the DT-DPP polymers containing dibenzothiophene, benzodithiophene, and bisthiophene (c, d, and e), whereas for the other DT-DPP polymers (a, b, and f) these are larger, up to 30 nm.

In Figure 6, we plot the value of maximum EQE for wavelength region λ > 700 nm where the polymer absorption dominates versus the average fibril width obtained from the TEM images (Table 2). Wider fibrils result in lower EQEs. For the blends with a fibril width less than 12 nm, the EQE is higher than 40% in the spectral region were the polymer absorbs, whereas for the materials with the wider fibrils (15−30 nm) the EQE is significantly less. It would have been interesting to change the fibril width of one DT-DPP polymer by changing the processing conditions and see the effect on EQE. In the SI, we show for all six polymers that the EQE is quite insensitive to the concentration of cosolvent in chloroform (Figures S8−S13, Tables S5−S10), which precludes such experiment. On the other hand, the correlation among the DT-DPP polymers corroborates with our recent work in which the PDPPTPT and PDPP3T polymers with different side chains (HD, OD, and DT) were studied.[34] The previous data are included in Figure 6 and reveal a remarkable good correlation with the new data presented here. The two open circles and the data point labeled with (a) are for HD-, OD-, and DT-PDPPTPT, and the open square and the data

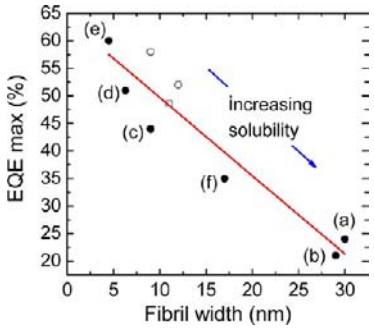

Figure 6. Plot of the maximum EQE in the high wavelength region (λ > 700 nm) versus the average fibril width for each of the DT-DPP polymers (marked with (a)−(f); see also Figure 5). The open markers are the results reported in ref 34 for PDPPTPT (open circles: HD, OD; (a) DT side chains) and PDPP3T (open square: HD; (b) DT side chains). The line is a guide to the eye.

point labeled with (b) are for HD- and DT-PDPP3T, respectively. Because the HD-, OD-, and DT-PDPPTPTs have the same optical gap, energy levels, and charge carrier mobilities,[34] the different performance is most likely due to a change in morphology, that is, the fibril width.

The optimized cells of DT-PDPP3T and DT-PDPP2T-TT with [70]PCBM are significantly thicker (220−240 nm) than those for the other DT-DPP polymers (90−115 nm) (Table 2). In the SI (Figures S3 and S4), we show that for DT-PDPP3T and DT-PDPP2T-TT the EQE in the wavelength region λ > 700 nm (where the polymer absorbs) is fairly insensitive to the film thickness for d > 100 nm. Figures S3 and S4 show that the increased PCE for thicker films is primarily due to a larger contribution of absorption of light by [70]PCBM. For this reason, the correlation between PCE and fibril width (w) is less outspoken than that between w and EQE. Other effects that complicate correlating PCE and fibril width are differences in FF (significantly smaller for DT-PDPPTPT) and differences in the photon energy loss, defined as $E_g - eV_{oc}$. A larger photon energy loss implies that the V_{oc} is unoptimized compared to the band gap. Among the DT-DPP polymers, the photon energy loss $E_g - eV_{oc}$ is larger for DT-PDPP2T-DBT than for the other materials.

The relation between fibril width and EQE can be rationalized by considering the fate of excitons that are generated in such semicrystalline polymer fibers. If the exciton is generated at the interface of the fiber with the fullerenes in the surrounding matrix, it can easily dissociate into electrons and holes by a photoinduced electron transfer reaction. Also excitons generated inside the fiber at short distances from this interface can contribute to charge generation after diffusing to the interface. The short singlet excited state lifetime (<100 ps) of DPP-based polymers, however, will limit the average exciton diffusion length to a few nanometers.[35] This will cause a reduction in charge generation efficiency when the fibril width becomes larger than (twice) the average exciton diffusion length. In our previous study on PDPPTPT derivatives, we were able to support this mechanism by showing that the fluorescence quenching in PDPPTPT:[70]PCBM blends is less for wider fibrils.[34]

Of course, other factors than the fibril width can contribute to determining the EQE, and it is useful to consider these briefly. First, differences in charge carrier mobility can play a role in geminate recombination of charges at the donor−acceptor interface and in bimolecular recombination after separation. The J−V characteristics of the DT-DPP:[70]PCBM solar cells show, however, a negligible increase in photocurrent under reverse bias

dx.doi.org/10.1021/ja4101003 | J. Am. Chem. Soc. 2013, 135, 18942−18948

(Figure 4a) and good to excellent fill factors. This suggests that differences in geminate and nongeminate recombination of charges are not the main factors that contribute to the differences in EQE. A second explanation could be the photon energy loss, defined as $E_g - eV_{oc}$. We have previously suggested that an increased photon energy loss can lead to a higher quantum efficiency for charge generation.[15] However, among the DT-DPP polymers, there is no clear relation between $E_g - eV_{oc}$ and the EQE (SI Figure S7). Actually, the EQEs of 0.52 for DT-PDPPBDT and 0.60 for DT-PDPP4T are high considering that their photon energy losses of 0.67 and 0.76 eV are close to the 0.6 eV considered as a minimal for charge generation,[36] and exceed the previous limits found for DPP-based polymers (Figure S7).

We conclude that the width of the DPP-based polymer fibers is an important factor contributing to the efficiency of charge generation. This width is controlled by the solubility of the polymer, which in turn depends on the structure of the conjugated backbone, the length of the side chains, and the degree of polymerization. In our experience, it is important to search for the limits of solubility, either by decreasing the length or number of side chains or by increasing the molecular weight. The solubility of these polymers seems a simple parameter, but in practice it is difficult to determine because in solution these high-molecular-weight polymers can be dissolved in a continuum of states that continuously interconvert: as single polymers chains, as aggregated chains or fibers, and as gels. At present, we can only speculate about mechanism how solubility controls the fiber width. A possible explanation is that the enhanced solubility increases the time that chains remain mobile in the solution phase. This increases the possibility for the crystalline fibers to grow and hence wider fibers are formed.

3. CONCLUSIONS

High molecular weight diketopyrrolopyrrole-based conjugated polymers with 2′-decyltetradecyl substituents (DT-DPP) were synthesized that incorporate different electron-donating units in the main chain to tailor the electronic structure and solubility of the polymers. The DT-DPP-based polymers were applied in organic solar cells with [70]PCBM and show high PCEs over ∼7% for less soluble polymers and low PCEs down to ∼3% for more soluble materials. All high molecular weight DPP polymers investigated here form an extended semicrystalline fibrillar network in blends with [70]PCBM as evidenced from bright field TEM. We find that the width of the fibrils correlates with the EQE of photon-to-electron conversion. A prime parameter determining the width of the fibers is the solubility of the polymers. Comparison with other DPP-based polymers suggests that the relation between fiber width and EQE is almost universal for this class of materials. At present, it is an open question whether this relationship between EQE and fibril width can be extended to other systems. The tendency to form semicrystalline structures in blends with PCBM is a property that the DT-DPP polymers share with several successful conjugated polymers used for solar cells. As a consequence, the optimized dimensions of the pure semicrystalline domains will need a careful balance between being small enough to ensure efficient exciton dissociation and large enough to sustain charge separation and charge transport over the thickness of the active layers. This study shows that solubility, determined by the nature of the polymer backbone, the side chains, and the molecular weight, is an important parameter.

4. EXPERIMENTAL SECTION

Molecular weight was determined with GPC at 80 °C on a PL-GPC 120 system using a PL-GEL 10 μm MIXED-B column and *o*-DCB as the eluent against polystyrene standards. Electronic spectra were recorded on a Perkin-Elmer Lambda 900 UV/vis/nearIR spectrophotometer. Cyclic voltammetry was conducted with a scan rate of 0.1 V s^{-1} under an inert atmosphere with 1 M tetrabutylammonium hexafluorophosphate in *o*-DCB as the electrolyte. The working electrode was a platinum disk, and the counter electrode was a silver electrode. The concentration of the sample in the electrolyte was approximately 1 mM, based on monomers. An Ag/Ag^+ quasi-reference electrode was used with Fc/Fc^+ as an internal standard. AFM images were taken on a Veeco MultiMode atomic force microscope connected to a Nanoscope III controller operating in tapping mode using PPP-NCH-50 probes (Nanosensors). TEM was performed on a Tecnai G^2 Sphera transmission electron microscope (FEI) operated at 200 kV. Fibril widths were determined by measuring and averaging over a number of manually chosen positions in the TEM image of the blend films.

Photovoltaic devices were made by spin coating poly(ethylenedioxythiophene):poly(styrene sulfonate) (PEDOT:PSS) (Clevios P, VP Al 4083) onto precleaned, patterned indium tin oxide (ITO) substrates (14 Ω per square) (Naranjo Substrates). The photoactive layers were deposited by spin-coating a chloroform solution containing the polymers and [70]PCBM with different ratios and the appropriate amount of 1,8-diiodooctane (DIO) or *o*-DCB. LiF (1 nm) and Al (100 nm) were deposited by vacuum evaporation at $\sim 2 \times 10^{-7}$ mbar as the back electrode. The active area of the cells was 0.09 or 0.16 cm^2, and no size dependence was found between these two dimensions. *J*−*V* characteristics were measured under ∼100 mW cm^{-2} white light from a tungsten-halogen lamp filtered by a Schott GG385 UV filter and a Hoya LB 120 daylight filter, using a Keithley 2400 source meter. Short circuit currents under AM1.5G conditions were estimated from the spectral response and convolution with the solar spectrum. The spectral response was measured under simulated 1 sun operation conditions using bias light from a 532 nm solid state laser (Edmund Optics). Light from a 50 W tungsten halogen lamp (Osram64610) was used as probe light and modulated with a mechanical chopper before passing the monochromator (Oriel, Cornerstone 130) to select the wavelength. The response was recorded as the voltage over a 50 resistance, using a lock-in amplifier (Stanford Research Systems SR 830). A calibrated Si cell was used as reference. The device was kept behind a quartz window in a nitrogen filled container. The thickness of the active layers in the photovoltaic devices was measured on a Veeco Dektak 150 profilometer.

■ ASSOCIATED CONTENT

Ⓢ Supporting Information

Synthetic procedures for the polymers, optical properties, cyclic voltammograms, charge carrier mobility, effects of layer thickness, AFM images of DT-DPP polymer blends with [70]PCBM, EQE vs energy loss, and effect of the concentration and choice of co-solvent. This material is available free of charge via the Internet at http://pubs.acs.org.

■ AUTHOR INFORMATION

Corresponding Author

r.a.j.janssen@tue.nl

Notes

The authors declare no competing financial interest.

■ ACKNOWLEDGMENTS

We thank Ralf Bovee for GPC analysis. The work was performed in the framework of the Largecells and X10D projects that received funding from the European Commission's Seventh Framework Programme (Grant Agreement No. 261936 and No. 287818). The work was further supported by the "Europees Fonds voor Regionale Ontwikkeling" (EFRO) in the Interreg IV-

A project "Organext". The research forms part of the Solliance OPV programme and has received funding from the Ministry of Education, Culture and Science (Gravity program 024.001.035).

REFERENCES

(1) Wienk, M. M.; Turbiez, M.; Gilot, J.; Janssen, R. A. J. *Adv. Mater.* **2008**, *20*, 2556−2560.
(2) Bijleveld, J. C.; Zoombelt, A. P.; Mathijssen, S. G. J.; Wienk, M. M.; Turbiez, M.; de Leeuw, D. M.; Janssen, R. A. J. *J. Am. Chem. Soc.* **2009**, *131*, 16616−16617.
(3) Zhou, E.; Yamakawa, S.; Tajima, K.; Yang, C.; Hashimoto, K. *Chem. Mater.* **2009**, *21*, 4055−4061.
(4) Bijleveld, J. C.; Gevaerts, V. S.; Di Nuzzo, D.; Turbiez, M.; Mathijssen, S. G. J.; de Leeuw, D. M.; Wienk, M. M.; Janssen, R. A. J. *Adv. Mater.* **2010**, *22*, E242−E246.
(5) Zhang, G. B.; Fu, Y. Y.; Xie, Z. Y.; Zhang, Q. *Sol. Energy Mater. Sol. Cells* **2011**, *95*, 1168−1173.
(6) Bronstein, H.; Chen, Z. Y.; Ashraf, R. S.; Zhang, W. M.; Du, J. P.; Durrant, J. R.; Tuladhar, P. S.; Song, K.; Watkins, S. E.; Geerts, Y.; Wienk, M. M.; Janssen, R. A. J.; Anthopoulos, T.; Sirringhaus, H.; Heeney, M.; McCulloch, I. *J. Am. Chem. Soc.* **2011**, *133*, 3272−3275.
(7) Zhang, X.; Richter, L. J.; DeLongchamp, D. M.; Kline, R. J.; Hammond, M. R.; McCulloch, I.; Heeney, M.; Ashraf, R. S.; Smith, J. N.; Anthopoulos, T. D.; Schroeder, B.; Geerts, Y. H.; Fischer, D. A.; Toney, M. F. *J. Am. Chem. Soc.* **2011**, *133*, 15073−15084.
(8) Jung, J. W.; Jo, J. W.; Liu, F.; Russell, T. P.; Jo, W. H. *Chem. Commun.* **2012**, *48*, 6933−6935.
(9) Bijleveld, J. C.; Verstrijden, R. A. M.; Wienk, M. M.; Janssen, R. A. J. *J. Mater. Chem.* **2011**, *21*, 9224−9231.
(10) Liu, F.; Gu, Y.; Wang, C.; Zhao, W.; Chen, D.; Briseno, A. L.; Russell, T. P. *Adv. Mater.* **2012**, *24*, 3947−3951.
(11) Qu, S. Y.; Tian, H. *Chem. Commun.* **2012**, *48*, 3039−3051.
(12) Jung, J. W.; Jo, J. W.; Liu, F.; Russell, T. P.; Jo, W. H. *Chem. Commun.* **2012**, *48*, 6933−6935.
(13) Jung, J. W.; Liu, F.; Russell, T. P.; Jo, W. H. *Energy Environ. Sci.* **2012**, *5*, 6857−6861.
(14) Zhou, E. J.; Cong, J. Z.; Hashimoto, K.; Tajima, K. *Energy Environ. Sci.* **2012**, *5*, 9756−9759.
(15) Li, W. W.; Roelofs, W. S. C.; Wienk, M. A.; Janssen, R. A. J. *J. Am. Chem. Soc.* **2012**, *134*, 13787−13795.
(16) Yiu, A. T.; Beaujuge, P. M.; Lee, O. P.; Woo, C. H.; Toney, M. F.; Fréchet, J. M. J. *J. Am. Chem. Soc.* **2012**, *134*, 2180−2185.
(17) Liu, F.; Gu, Y.; Wang, C.; Zhao, W.; Chen, D.; Briseno, A. L.; Russell, T. P. *Adv. Mater.* **2012**, *24*, 3947−3951.
(18) Li, W. W.; Hendriks, K. H.; Roelofs, W. S. C.; Kim, Y.; Wienk, M. M.; Janssen, R. A. J. *Adv. Mater.* **2013**, *25*, 3182−3186.
(19) Hendriks, K. H.; Heintges, G. H. L.; Gevaerts, V. S.; Wienk, M. M.; Janssen, R. A. J. *Angew. Chem., Int. Ed.* **2013**, *52*, 8341−8344.
(20) Gilot, J.; Wienk, M. M.; Janssen, R. A. J. *Adv. Mater.* **2010**, *22*, E67−E71.
(21) Gilot, J.; Wienk, M. M.; Janssen, R. A. J. *Adv. Funct. Mater.* **2010**, *20*, 3904−3911.
(22) Gevaerts, V. S.; Furlan, A.; Wienk, M. M.; Turbiez, M.; Janssen, R. A. J. *Adv. Mater.* **2012**, *24*, 2130−2134.
(23) Kouijzer, S.; Esiner, S.; Frijters, C. H.; Turbiez, M.; Wienk, M. M.; Janssen, R. A. J. *Adv. Energy Mater.* **2012**, *2*, 945−949.
(24) Dou, L. T.; You, J. B.; Yang, J.; Chen, C. C.; He, Y. J.; Murase, S.; Moriarty, T.; Emery, K.; Li, G.; Yang, Y. *Nat. Photonics* **2012**, *6*, 180−185.
(25) Dou, L. T.; Gao, J.; Richard, E.; You, J. B.; Chen, C. C.; Cha, K. C.; He, Y. J.; Li, G.; Yang, Y. *J. Am. Chem. Soc.* **2012**, *134*, 10071−10079.
(26) Dou, L. T.; Chang, W. H.; Gao, J.; Chen, C. C.; You, J. B.; Yang, Y. *Adv. Mater.* **2013**, *25*, 825−831.
(27) Esiner, S.; van Eersel, H.; Wienk, M. M.; Janssen, R. A. J. *Adv. Mater.* **2013**, *25*, 2932−2936.
(28) Li, W. W.; Furlan, A.; Hendriks, K. H.; Wienk, M. M.; Janssen, R. A. J. *J. Am. Chem. Soc.* **2013**, *135*, 5529−5532.
(29) Bavel, S.; Veenstra, S.; Loos, J. *Macromol. Rapid Commun.* **2010**, *31*, 1835−1845.
(30) Brabec, C. J.; Heeney, M.; McCulloch, I.; Nelson, J. *Chem. Soc. Rev.* **2011**, *40*, 1185−1199.
(31) Liu, F.; Gu, Y.; Jung, J. W.; Jo, W. H.; Russell, T. P. *J. Polym. Sci., Part B* **2012**, *50*, 1018−1044.
(32) Ruderer, M. A.; Mueller-Buschbaum, P. *Soft Matter* **2011**, *7*, 5482−5493.
(33) Kouijzer, S.; Michels, J. J.; van den Berg, M.; Gevaerts, V. S.; Turbiez, M.; Wienk, M. M.; Janssen, R. A. J. *J. Am. Chem. Soc.* **2013**, *135*, 12057−12067.
(34) Li, W. W.; Hendriks, K. H.; Furlan, A.; Roelofs, W. S. C.; Meskers, S. C. J.; Wienk, M. M.; Janssen, R. A. J. *Adv. Mater.* **2013**, DOI: 10.1002/adma.201304360.
(35) Markov, D. E.; Amsterdam, E.; Blom, P. W. M.; Sieval, A. B.; Hummelen, J. C. *J. Phys. Chem. A* **2005**, *109*, 5266−5274.
(36) Veldman, D.; İpek, Ö.; Meskers, S. C. J.; Sweelssen, J.; Koetse, M. M.; Veenstra, S. C.; Kroon, J. M.; van Bavel, S. S.; Loos, J.; Janssen, R. A. J. *J. Am. Chem. Soc.* **2008**, *130*, 7721−7735.